

Role of Edge Magnetic Shear on the Limiter H -Mode Transition of the JIPP T-IIU Tokamak

K. Toi, K. Kawahata, S. Morita, T. Watari, R. Kumazawa, K. Ida, A. Ando, Y. Oka, M. Sakamoto, Y. Hamada, K. Adati, R. Ando, T. Aoki, S. Hidekuma, S. Hirokura, O. Kaneko, A. Karita, T. Kawamoto, Y. Kawasumi, T. Kuroda, K. Masai, K. Narihara, Y. Ogawa, K. Ohkubo, S. Okajima,^(a) T. Ozaki, M. Sasao, K. N. Sato, T. Seki, F. Shimpo, H. Takahashi, S. Tanahashi, Y. Taniguchi, and T. Tsuzuki

National Institute for Fusion Science, Nagoya 464-01, Japan

(Received 20 March 1989)

In a circular cross-section plasma bounded by a limiter, the H -mode transition is triggered by a rapid rampdown in plasma current during auxiliary heating, even in the case when the edge electron temperature gradually decreases prior to the transition. This result suggests that the transition is governed by the enhancement of the magnetic shear near the plasma edge, associated with the radial modification of the edge current-density profile.

PACS numbers: 52.55.Fa, 52.55.Pi

In the divertor configuration of the ASDEX tokamak,¹ it was discovered that auxiliary-heated plasmas can take two distinctly different confinement regimes: the usual degraded regime, L mode, and the newly observed improved regime, H mode. Later, this phenomenon was observed in other divertor tokamaks.²⁻⁵ In most of the H -mode discharges, the transition seems to occur when there is an appreciable rise in the edge electron temperature (T_{eb}) above a certain threshold.⁶ Moreover, a transport barrier with steep ∇T_e and ∇n_e is formed just inside the separatrix, where the global magnetic shear $\hat{s}_m = d \ln q / d \ln r$, with q the safety factor, increases significantly.⁷ Recent theory predicts that the increased shear provided by the *divertor configuration* may suppress edge turbulence and trigger the H -mode transition.⁸ It is thought that (i) *high edge magnetic shear*, \hat{s}_{mb} , and (ii) *high T_{eb}* may be important factors in determining the transition. However, observation of the transition in limiter-bounded plasmas with circular cross section⁹⁻¹¹ requires a reexamination of the role of \hat{s}_{mb} for the transition. The role of high T_{eb} should also be reconsidered, since in DIII-D (Ref. 12) there is only a small rise in T_{eb} across the transition in contrast to a large rise in the edge electron density, and since new data from ASDEX (Ref. 13) suggest the importance of the current-density profile near the edge, rather than T_{eb} . A limiter configuration may be advantageous for studying the role of the magnetic shear on the transition, because the shear can be changed simply by modifying the current-density profile with the same external magnetic configuration. In this Letter, we demonstrate for the first time that the rapid rampdown in plasma current (CRD) can easily trigger the transition, thus suggesting the importance of \hat{s}_{mb} even in the limiter H mode.

Two sets of aperture-type carbon limiters are mounted in the JIPP T-IIU tokamak¹⁴ (major radius $R \approx 91$ cm, minor radius $a \approx 23$ cm), displaced 180° toroidally from each other. The limiters, carbon tiles, and torus wall are conditioned by pulsed helium electron-cyclotron-resonance (ECR) discharge cleaning¹⁵ for about two

weeks with a 0.1-Hz repetition rate and by numerous tokamak conditioning discharges. We also use titanium gettering between shots to suppress the unfavorable density rise during auxiliary heating. A deuterium plasma with a hydrogen minority ($\sim 10\%$) is heated by ion-cyclotron range of frequency (ICRF) power $P_{rf} \lesssim 2.5$ MW and by nearly perpendicular neutral-beam injection (NI) $P_{NI} \lesssim 0.7$ MW. The electron-temperature (T_e), the density (n_e), and the ion-temperature profiles are measured by a ten-channel grating polychromator for electron-cyclotron-emission measurements,¹⁶ a six-channel HCN-laser interferometer,¹⁷ and a 50-channel charge-exchange recombination spectrometer (CXRS),¹⁸ respectively. The H_α, D_α emission (I_α) is monitored at four toroidal locations, and at one of these it is measured over the poloidal cross section by a twelve-channel photomultiplier array.¹⁹ The observed H mode exhibits characteristics of the divertor H mode, i.e., a sharp depression in I_α , a rapid rise in T_{eb} , an obvious rise in the central line-averaged electron density (\bar{n}_e^0), a sudden decrease in the scrapeoff-layer density, and the appearance of edge localized modes (ELM).²⁰ There is, however, no obvious rise in ion temperature across the transition, presumably due to the poor time resolution of the CXRS (≈ 17 ms), compared to the ELM frequency. The improvement in stored plasma energy W_p is clear, but not significant ($\sim 10\%$ – 15%).

Figure 1 shows a typical limiter H -mode discharge (solid curves) triggered by current rampdown, which is done by the application of a reversed loop voltage. The heating power is $P_{rf} \approx 1.3$ MW; the transition never occurs at this power level unless CRD is employed (dashed curves). In the lower traces of Fig. 1 with the expanded time scale, we compare the time evolution of T_{eb} (at $r/a \approx 0.83$) in the H mode obtained by CRD and in the L mode without CRD. As shown by arrows on the lower traces, T_{eb} in the L mode increases at each sawtooth event, becoming about 15% higher than the value of T_{eb} at the transition in the H mode. This indicates that the transition is not necessarily determined by

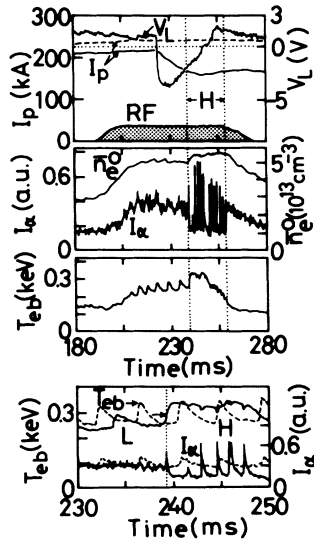


FIG. 1. Time evolution of the loop voltage (V_L), plasma current (I_p), H_{α} , D_{α} emission observed horizontally (I_{α}), line-averaged electron density along a central chord (\bar{n}_e^0), and edge electron temperature (T_{eb}) at $r/a \approx 0.83$ in a limiter H mode triggered by CRD, with $P_{rf} \approx 1.3$ MW and $B_t \approx 2.8$ T. The solid curves in the lower traces with the expanded time scale denote the H mode, and the dashed curves the L mode, whose I_p is shown by the dashed curve in the top trace.

T_{eb} .

We study which of the two possible effects, (a) the decreased plasma current, or (b) the radial modification of the current-density (j_{ϕ}) profile through the skin effect, is dominantly responsible for the H -mode transition by CRD. The dependence of the heating power $P_{rf} + P_{NI}$ on the plasma current I_p at the transition is shown in Fig. 2. This was obtained by varying the ICRF power from $P_{rf} \approx 0.5$ to ≈ 2.5 MW for fixed \bar{n}_e^0 [$\approx (5-6) \times 10^{13}$ cm^{-3}], B_t ($\approx 2.8-2.9$ T), and P_{NI} ($=0$ or ≈ 0.7 MW). The solid symbols in Fig. 2 indicate the data obtained with CRD, and the open symbols the data obtained without CRD (i.e., the constant- I_p case). The threshold P_{th} is defined as the minimum power required for the transition. For the H modes with CRD in the range of $I_p \gtrsim 170$ kA, a step-by-step scan of the heating power, which would determine P_{th} definitely, was not performed. Therefore, the broken curve shown in Fig. 2 may be higher than the value of P_{th} for this range of I_p . Nevertheless, it is lower by 30%–50% than the curve for the case without CRD. We conclude that the transition is determined not by the effect of decreased I_p , but by the modification of the edge j_{ϕ} profile. Note that $|\dot{I}_p|$ for CRD in this experiment is too small to lead to appreciable edge heating by a strongly reversed skin current.

To clarify the role of CRD on the H -mode transition, it is necessary to determine the location of the transport barrier formed near the plasma edge.⁷ The barrier is characterized as the region with steep ∇n_e and ∇T_e . The chord-averaged electron densities (\bar{n}_e) measured by the

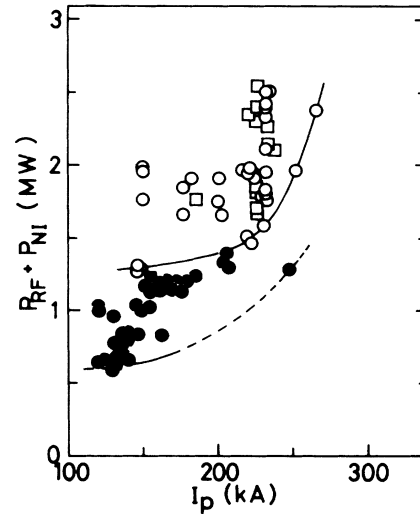


FIG. 2. Dependence of the total heating power on the plasma current at the moment of the H -mode transition. Circles, rf alone; squares, rf + NI. Solid symbols, with CRD; open symbols, without CRD.

six-channel HCN-laser interferometer suddenly rise or decrease just after the transition, depending on the location of the measuring chord. Figure 3 shows the radial variation of the relative change in the density $\Delta \bar{n}_e / \bar{n}_e$ for each measuring chord, in several H -mode discharges with CRD. From this figure, the location of the transport barrier may be determined as the position of $\Delta \bar{n}_e / \bar{n}_e = 0$. However, the position defined by $\Delta \bar{n}_e / \bar{n}_e = 0$ gives only a lower bound on the location of the barrier, because \bar{n}_e is the value of the density averaged along the measuring chord. This lower bound is $r/a \approx 0.70-0.80$.

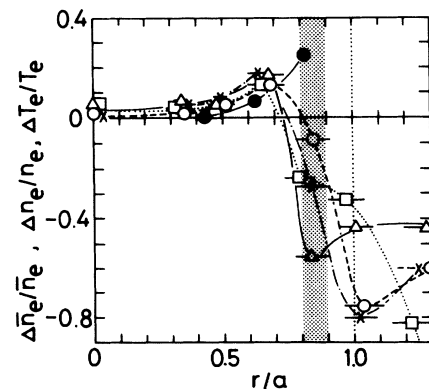


FIG. 3. Radial variation of the relative change in the chord-averaged density \bar{n}_e across the transition, in the H modes with CRD, where the applied loop voltage is in the range of -8.1 to -4.5 V and $P_{rf} \approx 1.1-1.3$ MW. The data at $r/a \approx 1.2-1.3$ are obtained by Langmuir probes. The shaded strip at $r/a = 0.8-0.9$ shows the location of the transport barrier determined from the Abel-inverted signals of interferometer. The relative change in T_e across the transition is shown by the solid circles.

The true location of the barrier has been determined by Abel inversion of the chord-integrated signals and is estimated to be $r/a \approx 0.80-0.90$ (shaded strip in Fig. 3). Figure 3 also shows the relative change in the electron temperature across the transition, which is estimated as the increment of T_e just prior to the first ELM of the H phase compared to the value of T_e just before the last sawtooth event in the L phase, divided by the latter value of T_e . The region with steep ∇T_e roughly coincides with the location of the barrier determined by the density measurements. We conclude that the transport barrier is formed near the plasma edge, but inside the limiter radius.

Figure 4 shows another typical H mode with CRD, where T_{eb} still does not govern the transition. For this H mode in a relatively high-density regime, T_{eb} reaches a maximum (indicated by the arrow) and decreases gradually until the transition. It is obvious that the transition is initiated without any sawtooth event and without any rise in T_{eb} prior to the transition. This result suggests that the transition is governed by the CRD-induced modification of the j_ϕ profile, instead of by T_{eb} . Note that high T_{eb} is necessary to well localize the CRD-induced skin effect near the edge, of which skin effect readily triggers the transition.

We estimate the magnetic shear by solving the magnetic diffusion equation with experimentally obtained

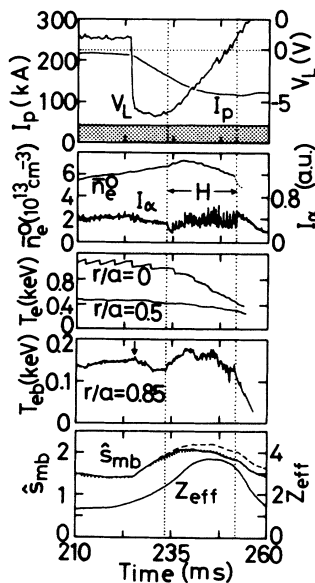


FIG. 4. H mode triggered by CRD without any sawtooth event and without any T_{eb} rise prior to the transition, where the shaded strip shows the heating pulse of $P_{rf} \approx 1.3$ MW plus $P_{NI} \approx 0.6$ MW. An arrow on T_{eb} trace indicates its maximum in the L phase. \hat{s}_{mb} is the shear calculated at $r/a=0.8$ for three Z_{eff} values, assuming the uniform profile: for experimentally obtained Z_{eff} (solid curve), and for the assumed $Z_{eff}=1.5$ (dashed curve) and $Z_{eff}=3.0$ (dotted curve). $T_e(a)=50$ eV and $n_e(a)=3 \times 10^{12}$ cm^{-3} are assumed at the limiter position.

data such as the I_p and the T_e and n_e profiles, adjusting the Z_{eff} profile so that the calculated loop voltage and the location of the $q=1$ surface agree well with the measured ones. Fairly good agreement with the experimental data is obtained for a uniform profile with $Z_{eff} \approx 2$ in this experiment. The time behavior of \hat{s}_{mb} depends weakly on the Z_{eff} value in the range of $1.5 \lesssim Z_{eff} \lesssim 3.0$, which is inferred from measurements of the visible bremsstrahlung, because the j_ϕ profile during CRD is determined predominantly by inductive effects rather than by resistive effects. Note that the time behavior of the internal inductance l_i calculated for $1.5 \lesssim Z_{eff} \lesssim 3$ agrees well with the value for l_i obtained from $\beta_p + l_i/2$ (from Shafranov shift) and $\beta_{p\perp}$ (from diamagnetic measurements). The calculated shear near the edge is appreciably increased by CRD from the value in the usual j_ϕ profile. When the shear at $r/a=0.8$, where the transport barrier is located, increases above a certain minimum value $\hat{s}_{mb} \approx 1.8-2.0$, the transition readily occurs (Fig. 4). The minimum of \hat{s}_{mb} (estimated at $r/a=0.8$) required for the transition decreases as the heating power is increased. This result is interpreted to indicate that the high-shear region with $\hat{s}_{mb} \approx 1.8-2.0$ slightly moves towards the limiter away from $r/a=0.8$, rather than indicating that the required shear is reduced at any edge position. On the other hand, rapid current rampup, which increases the Ohmic input near the edge, easily quenches the H mode obtained at very high heating powers ($P_{rf} + P_{NI} \approx 2.6$ MW). This result is interpreted to indicate that the shear edge \hat{s}_{mb} is appreciably reduced by a current rampup.

We now consider whether the H mode without CRD, obtained with high heating power, is governed by the same mechanism as discussed above, i.e., shear. The plasma current I_p tends to increase when strong electron heating occurs or when an appreciable amount of bootstrap current is generated in the plasma volume by high-power heating on a time scale shorter than the resistive diffusion time of the plasma. Then, a reversed toroidal electric field may be induced near the plasma edge due to conservation of poloidal magnetic flux. This electric field may detach the current channel from the limiter, keeping I_p constant. Thus, the j_ϕ profile may have pedestal or steep ∇j_ϕ at the profile edge where the magnetic shear rapidly increases up to ~ 2 . This j_ϕ profile would not be produced by the shrinkage due to enhanced edge recycling. This modification of the edge j_ϕ profile may stabilize localized tearing modes whose resonant surfaces are located in the detached region ($0.8 \lesssim r/a < 1.0$ in this experiment), because $dj_\phi/dr=0$ and the shear is high ($\hat{s}_{mb} \approx 2$) there.²¹ In this H mode where $q(a) \approx 4$, we observe that coherent magnetic fluctuations ($m/n=3/1$) excited near the edge during the L phase are dramatically suppressed just prior to the transition. Similar behavior of the coherent magnetic fluctuations is observed also in the divertor H mode.¹³

In this Letter, we have elucidated the fact that the

limiter H -mode transition is readily triggered by the enhancement of global magnetic shear near the edge. The enhanced shear may suppress edge turbulence, as has been discussed theoretically.⁸ In the limiter configuration, the enhancement of \hat{s}_{mb} is considered to be relatively small, because the maximum achievable value \hat{s}_{mb} is ~ 2 . This may lead to a relatively small improvement in the energy confinement. In a divertor configuration, the region of very high shear may be easily destroyed by edge turbulence during the L phase. Under the circumstances, enhancement of the edge shear by the modification of the j_ϕ profile becomes important even in this configuration. If the edge turbulence is suppressed by the above mechanism, a region of very high shear near the separatrix may be restored. Therefore, a large enhancement of \hat{s}_{mb} may be expected, which could lead to significantly improved confinement. On the other hand, recently developed theories,²²⁻²⁴ discussing the role of radial electric (E_r) field on plasma transport, would predict that a poloidal gyroradius increased by CRD would further obtain the H mode. However, they would not explain that the H mode is obtained much easier by CRD than by low I_p without CRD (Fig. 2). We need a direct measurement of the E_r field to draw the definite conclusion. As discussed above, we speculate that modification of the j_ϕ profile near the edge governs the H -mode transition also in divertor configuration as well as in limiter configuration. How the interior magnetic shear affects the confinement is still an open question.

The authors thank Professor K. Matsuura, Professor T. Sato, Professor A. Mohri, Professor H. Ikegami, Professor J. Fujita, Professor M. Fujiwara, and Professor A. Iiyoshi for their continual encouragement. They also thank Dr. J. Van Dam for his critical reading of the manuscript.

^(a)Permanent address: Department of Applied Physics, Chubu University, Kasugai 487, Japan.

¹F. Wagner *et al.*, Phys. Rev. Lett. **49**, 1408 (1982).

²R. Fonck *et al.*, in *Proceedings of the Fourth International Symposium on Heating of Toroidal Plasmas, Rome, 1984*,

edited by H. Knoepfel and E. Sindoni (International School of Plasma Physics, Varenna, 1984), p. 37.

³J. Luxon *et al.*, in *Proceedings of the Eleventh International Conference on Plasma Physics and Controlled Nuclear Fusion Research, Kyoto, 1986*, edited by J. W. Weil and M. Demir (International Atomic Energy Agency, Vienna, 1987), Vol. 1, p. 159.

⁴A. Tanga *et al.*, in *Proceedings of the Eleventh International Conference on Plasma Physics and Controlled Nuclear Fusion Research, Kyoto, 1986* (Ref. 3), p. 65.

⁵K. Odajima *et al.*, in *Proceedings of the Eleventh International Conference on Plasma Physics and Controlled Nuclear Fusion Research, Kyoto, 1986* (Ref. 3), p. 151.

⁶F. Wagner *et al.*, J. Nucl. Mater. **121**, 103 (1984).

⁷F. Wagner *et al.*, Phys. Rev. Lett. **53**, 1453 (1984).

⁸T. S. Hahm and P. H. Diamond, Phys. Fluids **30**, 133 (1987).

⁹H. Matsumoto *et al.*, in *Proceedings of the Fourteenth European Conference on Controlled Fusion and Plasma Physics, Madrid, Spain, 1987*, edited by S. Methfessel (European Physical Society, Petit-Lancy, Switzerland, 1987), p. 5.

¹⁰J. Manickam *et al.*, in *Proceedings of the Twelfth IAEA Conference on Plasma Physics and Controlled Nuclear Fusion Research, Nice, France, 1988* (International Atomic Energy Agency, Vienna, 1989), paper No. IAEA-CN-50/A-VII-4.

¹¹T. Watari *et al.*, Nucl. Fusion (to be published).

¹²J. Lohr *et al.*, Phys. Rev. Lett. **60**, 2630 (1988).

¹³K. Toi *et al.*, Phys. Rev. Lett. **62**, 430 (1989).

¹⁴K. Toi *et al.*, in *Proceedings of the Sixteenth European Conference on Controlled Fusion and Plasma Physics, Venice, 1989* (European Physical Society, Petit-Lancy, Switzerland, 1989), p. 221.

¹⁵H. R. Garner and T. Aoki, Fusion Technol. **9**, 481 (1986).

¹⁶K. W. Kawahata *et al.*, Jpn. J. Appl. Phys. **27**, 2349 (1988).

¹⁷K. Kawahata *et al.*, Rev. Sci. Instrum. **60**, 3734 (1989).

¹⁸K. Ida and S. Hidekuma, Rev. Sci. Instrum. **60**, 867 (1989).

¹⁹S. Morita, in *Proceedings of the U.S.-Japan Workshop on Evaluation of Impurity Pellet Injection for Alpha Diagnostics, San Diego, California, 1989* (unpublished).

²⁰M. Keilhacker *et al.*, Plasma Phys. Controlled Fusion **26**, 49 (1984).

²¹J. A. Wesson, Nucl. Fusion **18**, 87 (1978).

²²S. I. Itoh and K. Itoh, Phys. Rev. Lett. **60**, 2276 (1988).

²³K. C. Shaing and E. C. Crume, Phys. Rev. Lett. **63**, 2369 (1989).

²⁴H. Biglari *et al.*, Phys. Fluids B **2**, 1 (1990).

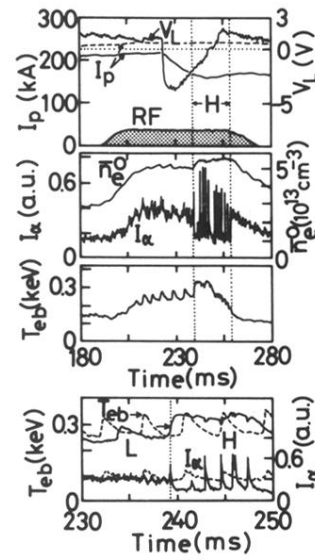


FIG. 1. Time evolution of the loop voltage (V_L), plasma current (I_p), H_α, D_α emission observed horizontally (I_α), line-averaged electron density along a central chord (\bar{n}_e^0), and edge electron temperature (T_{eb}) at $r/a \approx 0.83$ in a limiter H mode triggered by CRD, with $P_{rf} \approx 1.3$ MW and $B_t \approx 2.8$ T. The solid curves in the lower traces with the expanded time scale denote the H mode, and the dashed curves the L mode, whose I_p is shown by the dashed curve in the top trace.

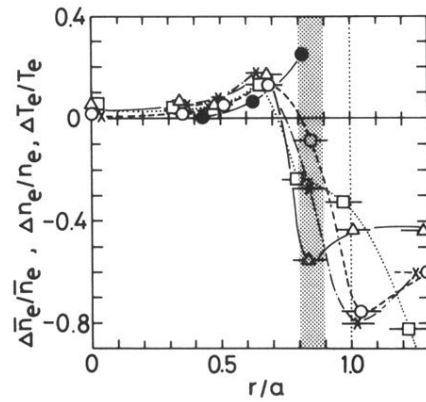


FIG. 3. Radial variation of the relative change in the chord-averaged density \bar{n}_e across the transition, in the H modes with CRD, where the applied loop voltage is in the range of -8.1 to -4.5 V and $P_{rf} \approx 1.1$ - 1.3 MW. The data at $r/a \approx 1.2$ - 1.3 are obtained by Langmuir probes. The shaded strip at $r/a = 0.8$ - 0.9 shows the location of the transport barrier determined from the Abel-inverted signals of interferometer. The relative change in T_e across the transition is shown by the solid circles.

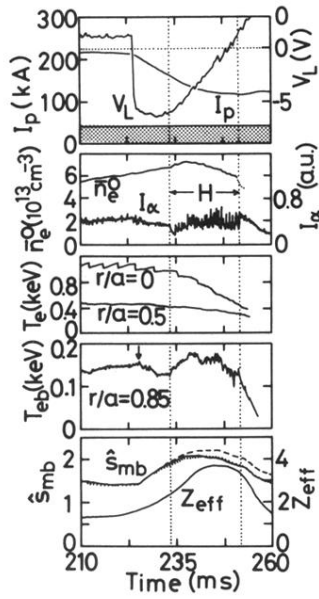


FIG. 4. H mode triggered by CRD without any sawtooth event and without any T_{eb} rise prior to the transition, where the shaded strip shows the heating pulse of $P_{rf} \approx 1.3$ MW plus $P_{NI} \approx 0.6$ MW. An arrow on T_{eb} trace indicates its maximum in the L phase. \hat{s}_{mb} is the shear calculated at $r/a = 0.8$ for three Z_{eff} values, assuming the uniform profile: for experimentally obtained Z_{eff} (solid curve), and for the assumed $Z_{eff} = 1.5$ (dashed curve) and $Z_{eff} = 3.0$ (dotted curve). $T_e(a) = 50$ eV and $n_e(a) = 3 \times 10^{12} \text{ cm}^{-3}$ are assumed at the limiter position.